

# Advances in Space Research

## A method of reconstruction of anisotropic fluxes of geomagnetically trapped particles from in-flight measurements of high precision

--Manuscript Draft--

<b>Manuscript Number:</b>	
<b>Article Type:</b>	EM -Earth Magnetosphere/Upper Atmosphere
<b>Keywords:</b>	Radiation belts Trapped radiation detection Partial acceptance Monte-Carlo simulations
<b>Corresponding Author:</b>	Alexey Anatolievich Leonov, Ph. D. Lebedev Physical Institute of the Russian Academy of Sciences Moscow, RUSSIAN FEDERATION
<b>First Author:</b>	Alexey Anatolievich Leonov, Ph. D.
<b>Order of Authors:</b>	Alexey Anatolievich Leonov, Ph. D. Vitaly Valerievich Malakhov Andrey Georgievich Mayorov, PhD Vladimir Vladimirovich Mikhailov, Professor Vladislav Vladimirovich Alekseev
<b>Abstract:</b>	<p>High anisotropy of geomagnetically trapped particles' fluxes requires utilization of a complex methodology for their reconstruction from in-flight measurements. For precise position-sensitive instruments operating in the event-by-event mode, a standard approach is the one originally developed for the SAMPEX/MAST experiment. It consists in calculation of the instrument's effective areas averaged over gyro-phase angle as a function of pitch angle of detected particles for detector's different orientations relative to the geomagnetic field vector. This orientation normally changes as the instrument moves in space. Moreover, some space vehicles bearing a measuring instrument may and do change their orientation during flight by rotation of the instrument or as a whole. Each possible orientation needs an independent calculation of effective areas for each possible pitch angle, which is usually done by means of Monte-Carlo simulation. Therefore, especially for sophisticated devices, the calculation of an accurate and representative response function (consisting of a set of effective areas) may involve a vast amount of computation.</p> <p>In this paper, we propose a simplified approach, which is based on the assumption that for an anisotropic flux, the angular sphere the particles come from to the detector can be split into solid angle domains, within which the flux can be treated as isotropic. This allows one to use much easier computed geometrical factor or acceptance of the instrument as the proportionality factor. This method suggests that it can be calculated with respect to registration of the particles from these domains (we call it partial acceptance). The main advantage of the presented method is that the whole set of partial acceptances for each instrument orientation relative to the geomagnetic field vector and for all available values of (equatorial) pitch-angle for this orientation can be obtained from one simulation sample (for the given energy) of isotropic flux.</p>
<b>Suggested Reviewers:</b>	<p>Stanislav Vladimirovich Borisov, PhD research assistant, Catholic University of Louvain, Belgium Stanislav.borisov@uclouvain.be Field of activity: development and data analysis of space radiation detectors (EPT, PROBA-V mission)</p> <p>Matteo Martucci, PhD full-time researcher, INFN Sezione di Roma "TorVergata", Italy Matteo.Martucci@roma2.infn.it Field of activity: cosmic rays (galactic, solar, trapped) study, experimental data processing and analysis (CSES-01 mission)</p>

	<p>Sergey Aleksandrovich Koldobskiy, PhD reseacher, University of Oulu, Finland sergey.koldobskiy@oulu.fi Field of activity: cosmic rays study, experimental data processing</p>
--	--

# A method of reconstruction of anisotropic fluxes of geomagnetically trapped particles from in-flight measurements of high precision

A.A. Leonov<sup>a,b</sup>, V.V. Malakhov<sup>b</sup>, A.G. Mayorov<sup>b</sup>, V.V. Mikhailov<sup>c</sup>, V.V. Alekseev<sup>d</sup>

<sup>a</sup>*Lebedev Physical Institute, Moscow 119991, Russia*

<sup>b</sup>*National Research Nuclear University MEPhI, Moscow 115409, Russia*

<sup>c</sup>*Shandong Institute of advanced technology, Jinan, 250014, China*

<sup>d</sup>*Demidov Yaroslavl State University, Yaroslavl, 150003, Russia*

## Abstract

High anisotropy of geomagnetically trapped particles' fluxes requires utilization of a complex methodology for their reconstruction from in-flight measurements. For precise position-sensitive instruments operating in the event-by-event mode, a standard approach is the one originally developed for the SAMPEX/MAST experiment. It consists in calculation of the instrument's effective areas averaged over gyro-phase angle as a function of pitch angle of detected particles for detector's different orientations relative to the geomagnetic field vector. This orientation normally changes as the instrument moves in space. Moreover, some space vehicles bearing a measuring instrument may and do change their orientation during flight by rotation of the instrument or as a whole. Each possible orientation needs an independent calculation of effective areas for each possible pitch angle, which is usually done by means of Monte-Carlo simulation. Therefore, especially for sophisticated devices, the calculation of an accurate and representative response function (consisting of a set of effective areas) may involve a vast amount of computation.

In this paper, we propose a simplified approach, which is based on the assumption that for an anisotropic flux, the angular sphere the particles come from to the detector can be split into solid angle domains, within which the flux can be treated as isotropic. This allows one to use much easier computed geometrical factor or acceptance of the instrument as the proportionality factor. This method suggests that it can be calculated with respect to registration of the particles from these domains (we call it partial acceptance). The main advantage of the presented method is that the whole set of partial acceptances for each instrument orientation relative to the geomagnetic field vector and for all available values of (equatorial) pitch-angle for this orientation can be obtained from one simulation sample (for the given energy) of isotropic flux.

## 1. Introduction

At present, the nature of long-term geomagnetic trapping of protons is well understood (Selesnick, et al, 2007). The sources of trapped protons with energies of more than ~MeV are cosmic ray albedo neutron decay (CRAND) (Singer, 1958) and injected solar protons (Hudson, 2004; Mazur, et al, 2006). The latter prevail at energies <100 MeV and in the outer zone (McIlwain's parameter  $L$  (McIlwain, 1966)  $> 1.3$ ), while the former dominates otherwise. Inelastic nuclear scattering, energy transfer to free plasma electrons, and ionization of the neutral atmosphere provide the losses (Selesnick, et al, 2007).

It is well known that the fluxes of trapped protons at the lower edge of the radiation belt are highly anisotropic (Parker, 1957; Fisher, et al., 1977). For description of their angular dependence, an approximating function of the form  $F \sim \sin^\zeta \alpha_{eq}$  is used (Parker, 1957), where  $\alpha_{eq}$  is the equatorial pitch angle and  $\zeta$  is the anisotropy coefficient.  $\zeta$  varies significantly with  $L$ , e.g. from 12 at  $L=1.35$  to 60 at  $L=1.15$  for 5-50 MeV protons (Fisher, et al., 1977). This level of anisotropy results in fluxes rising exceptionally sharply with an increase in the pitch angle: up to one order of magnitude increase in the flux per  $4^\circ$  pitch-angle increase (Adriani, et al., 2015). For detailed observation of the fluxes within a small pitch-angle interval, high angular resolution is necessary. It is typically achieved in the position-sensitive detectors operating in the event-by-

event mode and able to reconstruct the incident particle's direction. The list of such instruments that carried out measurements in the Earth Inner Radiation Belt (IRB) includes the following experiments: SAMPEX/MAST (Cook, et al., 1993), NINA (Leonov, et al., 2005), NINA-2 (Leonov, et al., 2008), AMS (Fiandrini, et al., 2004), AMS-2 (Giovacchini, et al., 2015), PAMELA (Adriani, et al., 2015; Bruno, et al., 2021b), CSES-01 (Martucci, et al., 2022). To reconstruct the flux of trapped protons in these experiments (excluding both AMS spectrometers), the standard approach developed for the SAMPEX/MAST data has been utilized (Selesnick, et al., 1995). It implies calculation of the so-called effective areas, averaged over the gyrophase angle as a function of the pitch-angle for instrument's different orientations relative to the geomagnetic field vector. That means conducting a separate Monte-Carlo simulation for each orientation and each pitch-angle (and actually for each energy channel of the instrument), which requires considerable amount of computational resources and time, especially for sophisticated instruments. Besides, in the original method (Selesnick, et al., 1995) the averaging over gyro-angle values is applied, which is inconvenient to use at the boundary of the inner radiation belt, where the fluxes could be significantly dependent on gyro-angle (Bruno, et al., 2021a).

In this paper, we propose a simple and robust algorithm for the reconstruction of the trapped particles' fluxes from high spatial and high angular resolution measurements. It was tested on the PAMELA simulated and experimental data, but can be applied to other instruments from the list above or to future high precision experiments of this kind. The method suggests splitting the detector's field of view (FoV) into a set of solid angle domains (the minimal size of which is defined by the instrument's angular resolution), within which the flux can be considered isotropic. More specifically, the instrument's geometrical factor or acceptance (see the discussion about the term later in the text) for these domains turns out to be representative enough as a proportionality factor for the anisotropic flux reconstruction. The values of partial acceptance for each instrument orientation relative to the geomagnetic field vector and for a given pitch angle range are calculated from one simulation sample (for a given energy) in which initial particles are distributed isotopically over the instrument's FoV. The basics of the method have already been outlined in (Malakhov & A.G. Mayorov, 2021; Malakhov, et al., 2023, Malakhov, et al., 2024). Here, we provide a detailed description of the method as well as the verification and validation tests.

## 2. PAMELA measurements in the Earth's inner radiation belt

The PAMELA is a space-based spectrometer designed to study charged cosmic particles in the energy range from some tens of MeV up to several hundreds of GeV (Adriani, et al., 2014). The instrument operated on board the Resurs-DK1 satellite from the middle of 2006 until the beginning of 2016. The spacecraft had a semi-polar (70° inclination) and elliptical (350 – 610 km altitude) orbit and was three-axis stabilized. The satellite's orientation was calculated by the onboard processor using the information from the star trackers with an accuracy of under 1° (Picozza, et al., 2007). This, together with a high angular resolution of the PAMELA spectrometer (0.1-2.5° depending on energy), allows measuring the incident particle direction with high precision. This feature is unique for measurements in the IRB.

The satellite crossed the inner edge of the IRB in the South Atlantic Anomaly (SAA) region several times a day. The PAMELA spectrometer provided direct measurements of the trapped radiation at Mc'Ilwain parameter values  $L < 1.22$  and magnetic field values  $B < 0.216$  G. It is important to notice that the instrument avoided saturation in the region. Saturation in the event-by-event mode would have been characterized by the minimal or very close to the minimal value of livetime<sup>1</sup> attributed to a set of triggers following each other. An analysis showed that the minimum values are ascribed to only a few discontinuous triggers during any passage of SAA (Picozza, et al., 2007).

The results of the measurements of the geomagnetically trapped proton fluxes in the kinetic energy interval ranging from 80 MeV to the trapping limit (~2 GeV) performed by the PAMELA

---

<sup>1</sup> The minimal value of livetime is 0.16 ms.

mission at low Earth orbits (350 ÷ 610 km) and solar-cycle variations of these fluxes were reported in (Adriani, et al., 2015) and (Bruno, et al., 2021b), respectively. In these articles, energy, spatial and angular flux distributions and their temporal variations were investigated in detail using the effective area approach (Selesnick, et al., 1995).

### 3. Simplified method for the reconstruction of fluxes of geomagnetically trapped protons

An instrument's count rate is related to the flux through a scaling factor. The classical ones are the gathering power  $\Gamma$  and geometrical factor  $G$  introduced in (Sullivan, 1971). The former is applicable to any kind of flux while the latter – only to the isotropic one. Both depend on the instrument's geometry, and  $\Gamma$  also on the flux's characteristics. When evaluating flux inside the SAA region, an accurate calculation of  $\Gamma$  is crucial, because trapped radiation is highly anisotropic due to motion in an inhomogeneous magnetic field and the interaction with the Earth's atmosphere (Fisher, et al., 1977; Bruno, et al., 2021a). But gathering power  $\Gamma$  is not convenient and cannot be universal, therefore another parameter called effective area  $H$  was proposed by (Selesnick, et al., 1995). Hitherto, it has been used for calculation of trapped proton fluxes in PAMELA, as mentioned above, and CSES (Martucci, et al., 2022) experiments.

According to (Selesnick, et al., 1995), the number of trapped particles hitting the  $i$ -th energy bin from  $E_i$  to  $E_{i+1}$ ,  $k^{\text{th}}$  equatorial pitch-angle bin from  $\alpha_{eq,k}$  to  $\alpha_{eq,k+1}$ , and  $n^{\text{th}}$  L-shell bin from  $L_n$  to  $L_{n+1}$ , during the  $m^{\text{th}}$  temporal bin from  $t_m$  to  $t_{m+1}$ , is related to the flux intensity  $J(E, L, \alpha_{eq}, t)$  through the following expression:

$$N_{iknm} = \int_0^{2\pi} \int_{\alpha_{eq,k}}^{\alpha_{eq,k+1}} \int_{E_i}^{E_{i+1}} \int_{L_n < L < L_{n+1}}^{t_m}^{t_{m+1}} A(E, \theta(\alpha, \beta, \theta_B(t), \varphi_B(t)), \varphi(\alpha, \beta, \theta_B(t), \varphi_B(t))) \times \cos\theta(\alpha, \beta, \theta_B(t)) \times J(E, L, \alpha_{eq}, t) \times \sin\alpha \times \frac{d\alpha}{d\alpha_{eq}} \times dt dE d\alpha_{eq} d\beta \quad (1)$$

where the integral over  $t$  includes only the times when the spacecraft crossed the  $n$ -th L-shell bin;

$\alpha, \beta$  are the spherical angles of the incident particle velocity vector respective to the local magnetic field vector, i.e. the pitch angle and gyro angle, respectively;

$\theta_B(t), \varphi_B(t)$  are the spherical angles of the local magnetic field vector in the instrument reference frame (IRF);

$\theta, \varphi$  are the spherical angles of the incident particle velocity vector in the IRF;

$A(E, \theta(\alpha, \beta, \theta_B(t), \varphi_B(t)), \varphi(\alpha, \beta, \theta_B(t), \varphi_B(t)))$  is the detector's response function, which has units of area;

$\alpha_{eq}$  is the pitch angle of trapped particle at the geomagnetic equator, which is related to the local pitch angle  $\alpha$  through the first adiabatic invariant conservation law (Roederer, 1971).

It is worth mentioning that the flux  $J(E, L, \alpha_{eq}, t)$  in (1) also depends on gyro-phase angle  $\beta$ . At this point, an additional index for  $\beta$  bins could be added in (1), but this would only complicate the expression without apparent merits to the explanation. The flux  $J$  can be interpreted as a value, averaged over the range of gyro angles  $\beta$  overlapping the instrument's aperture.

The effective area, averaged over  $\beta$ , is then defined as follows:

$$H(E, \alpha, \theta_B, \varphi_B) = \frac{1}{2\pi} \int_0^{2\pi} A(E, \alpha, \beta, \theta_B, \varphi_B) \times \cos\theta(\alpha, \beta, \theta_B) \times \sin\alpha d\beta \quad (2)$$

The expression (1) holds on the assumption that the flux  $J_{i,k,m,n}$  is constant within i-k-n-m bin. The flux then is calculated in the following way:

$$J_{i,k,m,n} = N_{iknm} \times (2\pi \int_{\alpha_{eq,k}}^{\alpha_{eq,k+1}} \int_{E_i}^{E_{i+1}} \int_{L_n < L < L_{n+1}}^{t_m}^{t_{m+1}} H(E, \alpha(\alpha_{eq}, t), \theta_B(t), \varphi_B(t)) \frac{d\alpha}{d\alpha_{eq}} dt dE d\alpha_{eq})^{-1} \quad (3)$$

The scaling factor in this case is the expression in the denominator in equation (3). It depends on the pitch angle and the instrument's orientation ( $\theta_B, \varphi_B$ ) relative to the magnetic field, which in turn depends on time. Therefore, in practice, for an instrument with a typical orbit crossing IRB, a huge amount of Monte-Carlo simulation covering all possible values of  $\alpha, \theta_B, \varphi_B$  is necessary for an accurate calculation of the response function. The common practice assumes that the simulation is done for a set of pitch-angles and the instrument's orientations with some steps for which effective area  $H(E, \alpha, \theta_B, \varphi_B)$  is calculated, and intermediate values are interpolated.

In (Malakhov, et al., 2024) we proposed another quantity as a scaling factor, viz. partial geometrical factor  $G_{\Delta\alpha}$  relative to the registration of particles coming from the pitch-angle range  $\Delta\alpha$ :

$$G_{\Delta\alpha_l}(E, \theta_B, \varphi_B) = \int_{\alpha_k}^{\alpha_{k+1}} \int_0^{2\pi} A(E, \alpha, \beta, \theta_B, \varphi_B) \times \cos\theta(\alpha, \beta, \theta_B, \varphi_B) \times \sin\alpha \times d\alpha \times d\beta = 2\pi \int_{\alpha_k}^{\alpha_{k+1}} H d\alpha \quad (4)$$

where  $\Delta\alpha_k = \alpha_{k+1} - \alpha_k$  is a pitch-angle interval. One can see that it can be derived from the expression (2) by integration of the effective area  $H$  over pitch-angle.

It is evident that the partial geometrical factor is additive in angular space, i.e.  $G(E, \Delta\alpha_k + \Delta\alpha_{k+1}, \theta_B, \varphi_B) = G(E, \Delta\alpha_k, \theta_B, \varphi_B) + G(E, \Delta\alpha_{k+1}, \theta_B, \varphi_B)$ . The term *geometrical factor* may not be accurate, though, since it does not explicitly take into account the particles selection efficiency, i.e. the fact that in modern sophisticated instruments, a particle can be rejected from the analysis not just because its path does not fit into the instrument geometrically. Zhang, et al., 2011 suggested using the term *acceptance* for particle telescopes, which includes the selection efficiency  $\varepsilon$ , so basically it is  $G \times \varepsilon$ . We will use this entity further and for simplicity call  $G_{\Delta\alpha}$  a *partial acceptance* and imply that it includes  $\varepsilon$ .

Considering (4) and assuming that  $E_i$  and  $\alpha_k$  are independent within the intervals  $\Delta E_i$  and  $\Delta\alpha_k$  (which is achieved by the choice of the length of the intervals according to the instrument's angular and energetic resolution), expression (3) can be now rewritten as follows:

$$J_{i,k,m,n} = N_{iknm} \times \left( \int_{E_i}^{E_{i+1}} \int_{L_n < L < L_{n+1}}^{t_m} G_{\Delta\alpha_k \rightarrow \Delta\alpha_{eq,k}}(E, \theta_B, \varphi_B) \times dt dE \right)^{-1} \quad (5)$$

where  $G_{\Delta\alpha_k \rightarrow \Delta\alpha_{eq,k}}$  is the partial acceptance for the local pitch-angle interval  $\Delta\alpha_k$ , which corresponds to the chosen equatorial pitch-angle interval  $\Delta\alpha_{eq,k}$  through the first adiabatic invariant conservation law.

The value of the partial acceptance for any  $\Delta\alpha_k$  can be calculated from one sample of the isotropic flux simulation (Malakhov, et al., 2023; Malakhov, et al., 2024) in the usual way:

$$G_{\Delta\alpha_k}(E) = \frac{N_{\Delta\alpha_k}}{N_0(E)} \times \pi S \quad (6)$$

where  $N_0(E)$  is the total number of simulated particles;

$N_{\Delta\alpha_k}$  is the number of particles coming from  $\Delta\alpha_k$  pitch-angle band and survived selection criteria;  $S$  is the simulation surface area. Further for simplicity, we will omit  $k$ .

In Fig. 1 two examples of calculation of  $G_{\Delta\alpha}$  of 1 GV protons are shown for two different orientations of the PAMELA's instrumental reference frame (IRF) relative to the local magnetic field vector, characterized by  $\theta_B = 75^\circ, \varphi_B = 0^\circ$  (a) and  $\theta_B = 90^\circ, \varphi_B = 0^\circ$  (b), correspondingly. The light grey dots (forming the light grey continuous area on the plot) represent zenith and azimuthal angles of the reconstructed direction of the simulated protons that survived the standard selection criteria (Adriani, et al., 2011). The dark grey squares and black triangles forming curves depict the intersection of the PAMELA FoV cone and the local pitch angle cones of  $89^\circ$  and  $91^\circ$  opening angles, correspondingly.  $N_{\Delta\alpha}^{75^\circ}$  and  $N_{\Delta\alpha}^{90^\circ}$  are the numbers of selected protons found between these curves for the two aforementioned orientations, respectively. For both orientations, the values of



partial acceptance for this pitch-angle range can be calculated with (6) using the same simulation data sample. For the instrument orientation  $75^\circ$  the partial acceptance equals  $\sim 0.56 \text{ cm}^2 \times \text{sr}$ , for the instrument orientation  $90^\circ$  it is  $\sim 1.62 \text{ cm}^2 \times \text{sr}$ . One can see, that a  $15^\circ$  change in the orientation results in trebling of the  $G_{\Delta\alpha}$ . It is also obvious that the same simulation data sample can be used to calculate partial acceptance for any orientation and for any pitch-angle interval within which the flux is considered isotropic.

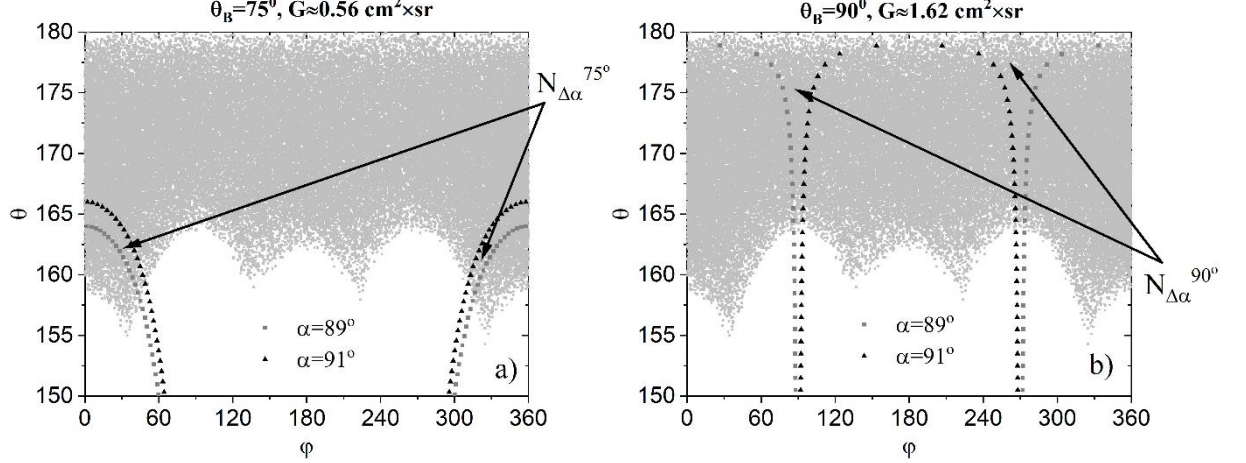


**Fig. 1.** The calculation of the partial acceptance for the instrument's axis orientations  $75^\circ$  (a) and  $90^\circ$  (b). The light grey dots (forming the light grey continuous area) represent zenith and azimuthal angles of the reconstructed direction of the simulated protons survived the standard selection criteria. The dark grey squares and black triangles forming curves depict the intersection of the PAMELA FoV cone and the local pitch angle cones  $89^\circ$  and  $91^\circ$  opening angles, correspondingly. The arrows indicate the region between the curves within which the numbers of selected protons  $N_{\Delta\alpha}^{75^\circ}$  (a) and  $N_{\Delta\alpha}^{90^\circ}$  (b) are counted.

#### 4. Verification tests

To examine the proposed method, we performed a couple of verification tests. At first, we checked if the algorithm can reproduce the simulated isotropic flux. For this purpose, an isotropic flux of protons of 1.5 GV passing through the PAMELA spectrometer from the upper hemisphere through the area S ( $62 \times 52 \text{ cm}^2$ ) placed right above the instrument has been simulated in two independent samples, each containing  $10^7$  events. One sample imitated the experimental data to measure ( $N_{\Delta\alpha}^{TEST}$ ), while the second one was used for calculation of the partial acceptance ( $N_{\Delta\alpha}^{BASIC}$ ).

From expression (6) one can see that  $G_{\Delta\alpha} \sim N_{\Delta\alpha}^{BASIC}$  and the flux  $J \sim \frac{N_{\Delta\alpha}^{TEST}}{G_{\Delta\alpha}} \sim \frac{N_{\Delta\alpha}^{TEST}}{N_{\Delta\alpha}^{BASIC}}$ .

Local pitch-angular distribution of the reconstructed flux was obtained relative to different designated directions, which emulated the direction of the magnetic field vector in the IRF. The available pitch-angle range was split into  $3^\circ$  bins. Figure 2 shows the flux distributions relative to the two directions characterized by  $\theta_B=85^\circ$ ,  $\phi_B=45^\circ$  (a) and by  $\theta_B=20^\circ$ ,  $\phi_B=0^\circ$  (b). The overall pitch-angle range was chosen in such a way that it overlaps the instrument FoV.

To check if the obtained flux distributions correspond to an isotropic flux, we performed two-sample Kolmogorov-Smirnov (KS) test, comparing  $N_{\Delta\alpha}^{BASIC}$  and  $N_{\Delta\alpha}^{TEST}$  samples for the two aforementioned orientations. KS statistic value is calculated as  $D_{mn} \sqrt{\frac{mn}{m+n}}$ , where  $D_{mn}$  is the maximal difference between the samples' empirical distribution functions,  $m$  and  $n$  are the sizes of the first and the second sample respectively. The test is passed at some significance level if the KS statistic value does not exceed a correspondent critical value of Kolmogorov distribution  $c$ . The results are shown in table 1, from which one can see that the both samples have passed the test at significance level 0.005 which means that they came from the same distribution. Considering that the test distribution corresponds to the isotropic flux we can conclude that the reconstructed distribution is isotropic too.

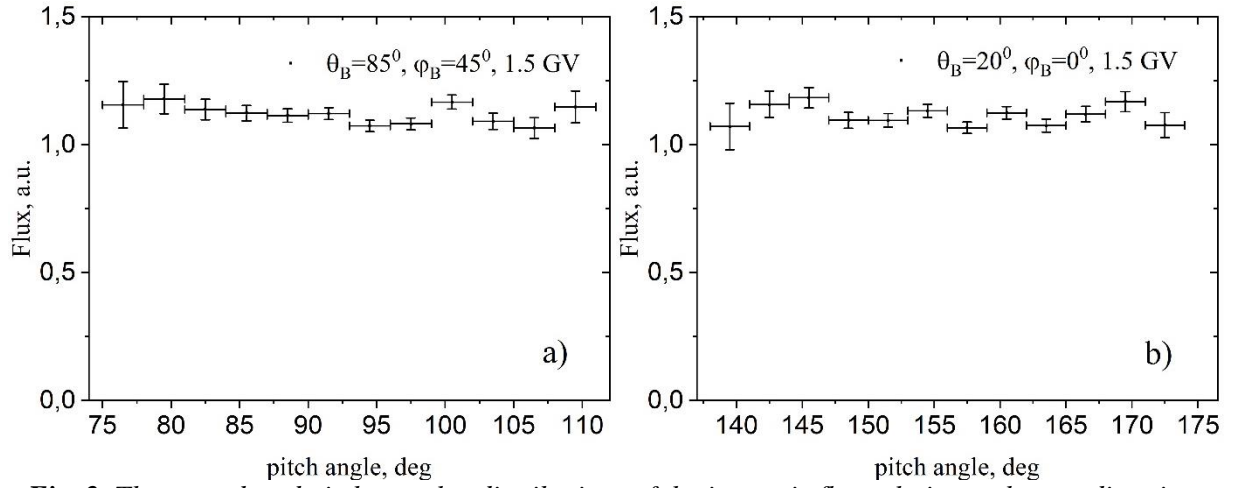


**Fig. 2.** The reproduced pitch-angular distributions of the isotropic flux relative to the two directions characterized by  $\theta_B=85^\circ$ ,  $\varphi_B=45^\circ$  (a) and  $\theta_B=20^\circ$ ,  $\varphi_B=0^\circ$  (b).

Dataset	$N^{TEST}$	$N^{BASIC}$	KS statistics value	$c$ (significance level 0.005)
Fig. 2a	32680	29419	0.742	1.358
Fig. 2b	32652	29432	0.611	1.358

**Table 1.** Results of two-sample Kolmogorov-Smirnov test.

Secondly, we checked if the algorithm can reconstruct an anisotropic (relative to an arbitrarily chosen direction in the IRF) flux with a given anisotropy index. For this test we simulated four independent samples of anisotropic flux of protons of 1.5 GV with the same simulation parameters (area of simulation surface  $S$  and solid angle  $\Omega$ ) but with different values of the anisotropy index  $\zeta$  and with different designated directions in the IRF. In the simulation, the initial pitch-angular dependence was set in a standard way as  $J \sim \sin^\zeta \alpha$ . For the calculation of the partial acceptances the previous sample of isotropic flux simulation was used.

To simulate an anisotropic flux, it is necessary to know a relative number of particles coming from different directions for a given anisotropy index. This number depends on the designated direction defined by spherical angles  $\theta_B$ ,  $\varphi_B$ , and anisotropy index  $A$  and can be described with the following probability function:

$$P \sim \cos\theta \times \sin^\zeta \alpha \times d\Omega_{\alpha\beta} = \cos\theta(\alpha, \beta, \theta_B) \times \sin^{\zeta+1} \alpha \times d\alpha \times d\beta \quad (7)$$

where

$$\cos\theta = -\sin\alpha \times \cos\beta \times \sin\theta_B + \cos\alpha \times \cos\theta_B \quad (8)$$

The azimuthal angle  $\varphi$  of the incident particle velocity vector in the IRF is calculated using the following relation:

$$\tan\varphi = \frac{\sin\alpha \times \cos\beta \times \cos\theta_B \times \sin\varphi_B + \sin\alpha \times \sin\beta \times \cos\varphi_B + \cos\alpha \times \sin\theta_B \times \sin\varphi_B}{\sin\alpha \times \cos\beta \times \cos\theta_B \times \cos\varphi_B - \sin\alpha \times \sin\beta \times \sin\varphi_B + \cos\alpha \times \sin\theta_B \times \cos\varphi_B} \quad (9)$$

The four simulation samples include three with the designated direction defined by  $\theta_B=90^\circ$ ,  $\varphi_B=0^\circ$  and  $\zeta = 20, 30$  and  $40$ ; and one sample defined by  $\theta_B=70^\circ$ ,  $\varphi_B=90^\circ$  and  $\zeta=40$ . In Fig. 3, a pitch-angular distributions of the partial acceptance, obtained by using the previous sample of isotropic flux simulation for orientations  $\theta_B = 90^\circ$ ,  $\varphi_B = 0^\circ$  (a) and for  $\theta_B = 70^\circ$ ,  $\varphi_B = 90^\circ$  (b) are shown (for this test, we split the available pitch-angle range into  $2^\circ$  bins). These values were applied in (5) while reconstructing the flux. Figure 4 shows the reproduced pitch-angular distribution of the flux in the four described cases. The dots indicate the reconstructed fluxes (all uncertainties are statistical) and the dashed lines are their approximations by the function  $f=\sin^\zeta \alpha$ . As one can see, the simulated and reconstructed anisotropy indices are in good agreement in all cases – even in the fourth (d), where the directions corresponding to the maximum of the pitch-angular distribution are not covered by the instrument's FoV. A high statistical uncertainty in the leftmost point is due to very small acceptance here and the resulting lack of selected events for the flux reconstruction.



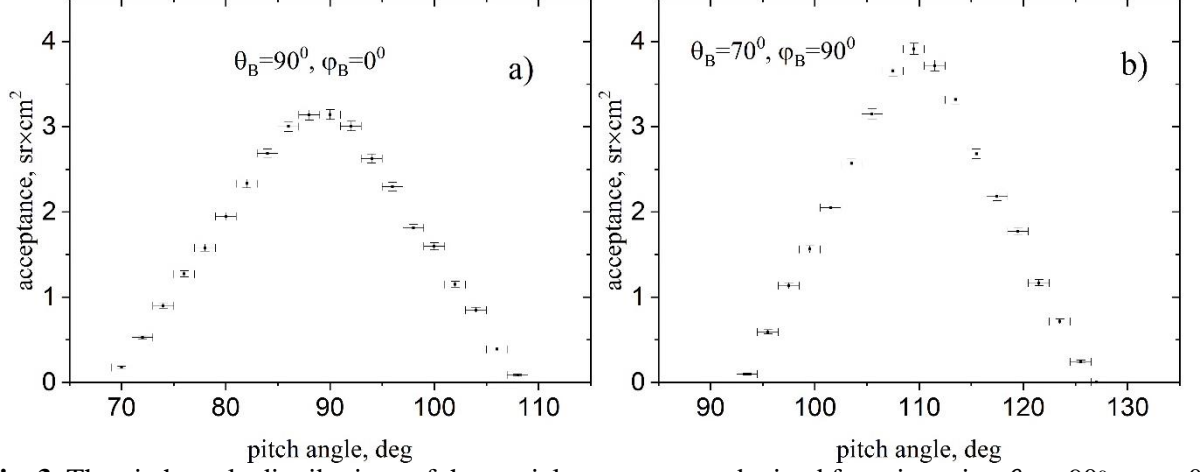


**Fig. 3.** The pitch angle distributions of the partial acceptances, obtained for orientation  $\theta_B = 90^\circ, \varphi_B = 0^\circ$  (a) and  $\theta_B = 70^\circ, \varphi_B = 90^\circ$  (b).

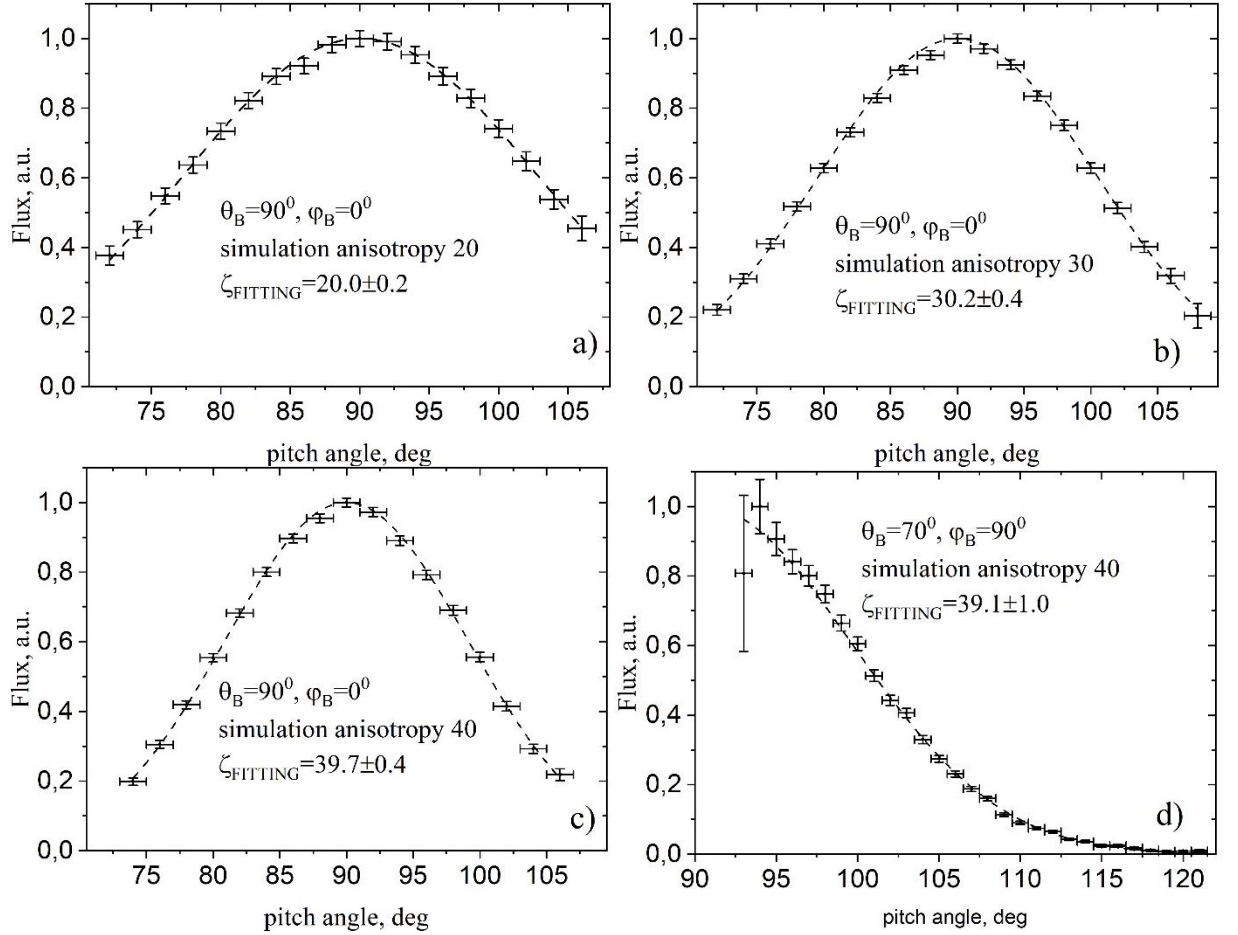


**Fig. 4.** Results of anisotropic flux reconstruction for orientation ( $\theta_B = 90^\circ, \varphi_B = 0^\circ$ ) and anisotropy indices 20 (a), 30 (b) and 40 (c) and for orientation ( $\theta_B = 70^\circ, \varphi_B = 90^\circ$ ) and anisotropy index 40 (d).

## 5. Validation tests

For the first validation test, we reconstructed pitch-angular distribution of galactic cosmic ray proton fluxes measured in the PAMELA experiment in rigidity range from 0.75 to 1.25 GV. The galactic component was selected using criterion  $L > 8$ . For calculation of the partial acceptance, we conducted the Monte-Carlo simulation of 1 GV protons. The direction relative to which the pitch-angular distributions of the fluxes were reconstructed was chosen arbitrarily in the IRF, because weak magnetic field does not affect the motion of particles significantly in this region. Figure 5 demonstrates a one-day GCR proton flux's pitch-angle distributions in arbitrary units.

These distributions were obtained relative to the directions  $\theta_B=20^\circ$ ,  $\varphi_B=0^\circ$  (a) and  $\theta_B=85^\circ$ ,  $\varphi_B=45^\circ$  (b).

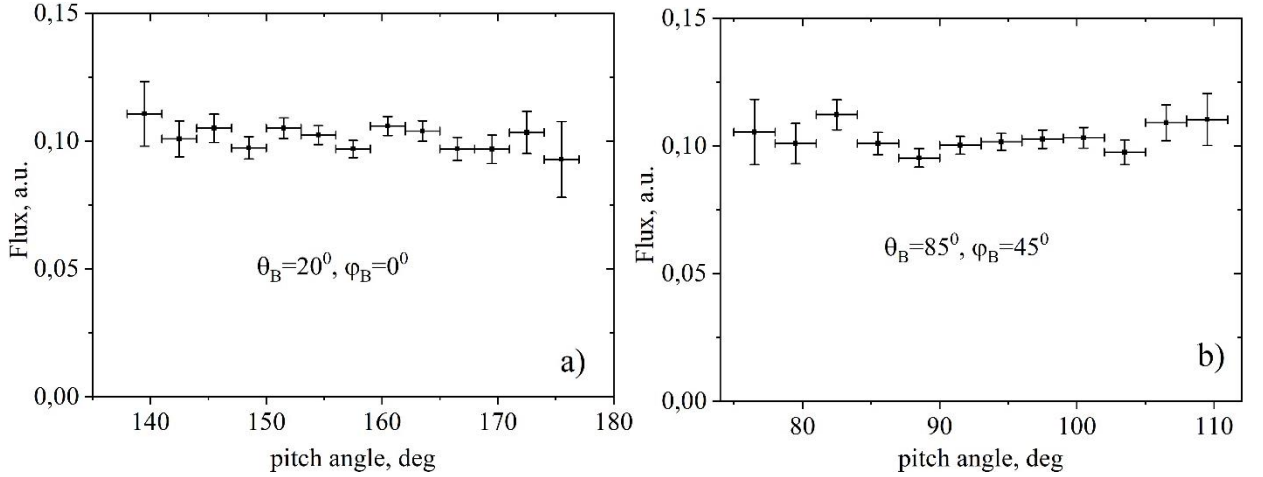


**Fig. 5.** Reconstructed a one-day GCR proton flux's pitch-angle distributions in arbitrary units. Distributions were obtained in a rigidity range from 0.75 to 1.25 GV relative to the directions  $\theta_B=20^\circ$ ,  $\varphi_B=0^\circ$  (a) and  $\theta_B=85^\circ$ ,  $\varphi_B=45^\circ$  (b).

To check if the distributions are isotropic, we again performed the KS-test comparing in this case number of experimentally registered events depending on  $\alpha$  for the two orientations and  $N_{\Delta\alpha}^{TEST}$  from the simulation. The results are shown in table 2 where one can conclude that in both cases the distributions correspond to an isotropic flux.

Dataset	$N^{GCR}$	$N^{BASIC}$	KS statistic value	c (significance level 0.005)
Fig. 5a	6471	63728	0.480	1.358
Fig. 5b	6418	63130	0.465	1.358

**Table 2.** Results of two-sample Kolmogorov-Smirnov test.

For the next validation test, we reconstructed short term proton fluxes trapped in the IRB using the PAMELA experimental data and compared it with the previous results obtained with the instrument using effective areas approach (Adriani, et al., 2015). For the new calculation we reprocessed the proton data, obtained in the L range from 1.145 to 1.155 along one passage through the IRB on two different days. For comparison, the equatorial pitch angles interval  $76-77^\circ$  was chosen. In figure 6, the proton energy spectra in the indicated pitch-angular and L ranges were reconstructed using the new method (triangles) for day 30.10.2006 (a) and for day 04.02.2007 are shown in comparison with the three years (2006-2009) spectrum published in (Adriani, et al, 2015) (dots). The figures show that both spectra are in good agreement.

Finally, we compared the equatorial pitch angular distributions obtained using the presented method with the data of NOAA-17 MEPED instrument. Figure 7 shows equatorial pitch-angle distributions of the proton fluxes in the energy range 70-140 MeV at  $L=1.16$  measured by NOAA-17 (grey dots) (Kuznetsov and Nikolayeva, 2012; <http://poes.ngdc.noaa.gov>) and obtained in this analysis from the PAMELA data (black dots). The data of NOAA-17 cover a one-month interval (April 2005), while our calculations are based on three months of data from July to September, 2006. One can see that there is good agreement between the data considering the instruments' characteristics and the measurements accuracies. Small discrepancies at certain points may be because NOAA-17 measured omnidirectional flux and assigned the pitch-angle of satellite's main axis to all of the currently detected events.

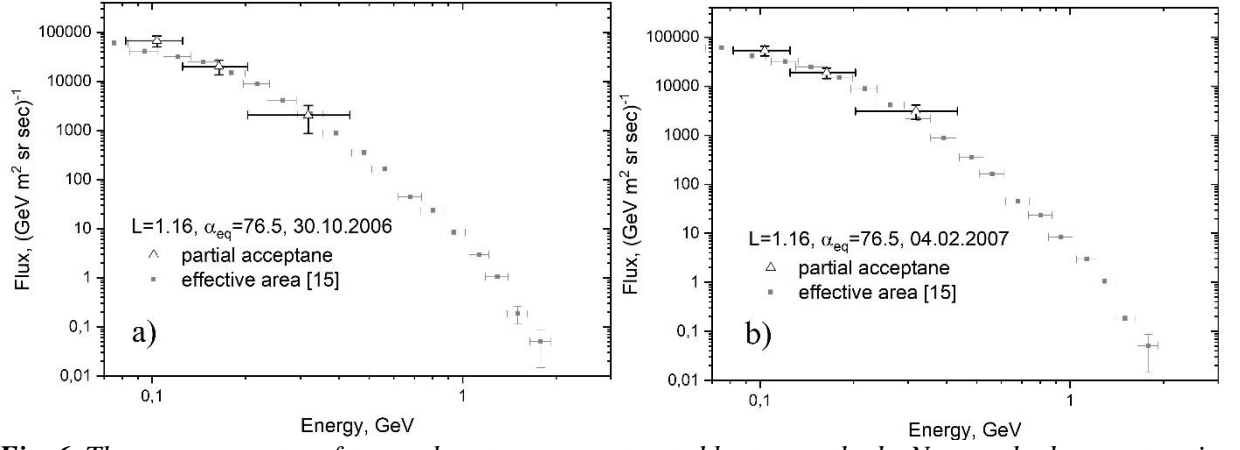


**Fig. 6.** The energy spectra of trapped protons reconstructed by two methods. New method reconstruction for the day 30.10.2006 (a) and for the day 04.02.2007 (b)

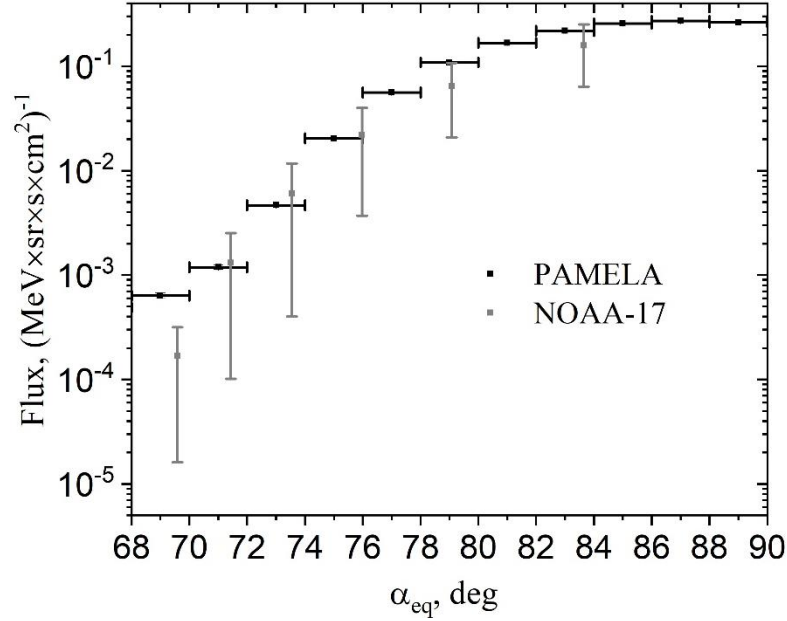


**Fig. 7.** Equatorial pitch-angle distributions of the proton flux in the energy range 70-140 MeV at  $L=1.16$  measured by NOAA-17 MEPED (grey dots) (Kuznetsov and Nikolayeva, 2012; <http://poes.ngdc.noaa.gov>) and obtained in this analysis from the PAMELA data (black dots). The data of NOAA-17 MEPED cover one-month interval (April 2005), while our calculations are based on three months of data from July to September, 2006.

## 6. Conclusion

A method of reconstruction of anisotropic fluxes of geomagnetically trapped protons applicable to direct in-orbit measurements of high spatial and energy resolution was proposed, realized and tested. The method is based on the calculation of the partial acceptance as a proportionality factor between the flux and count rate. The main distinction between our method and the common effective area approach is that the partial acceptance for any possible orientation and any possible pitch-angle range and binning can be calculated from a single simulation of an isotropic flux. The comparison with analogous results obtained using the effective area approach in the same energy,  $L$  and pitch-angle intervals showed a good agreement. The next step of the method development will be moving to the guiding center approximation, which will enable accurate reconstruction of fluxes at the energies up to  $\sim \text{GeV}$ , where geomagnetic parameters (especially  $L$ ) can differ significantly from their local values.

## Acknowledgments

We dedicate this paper to the kind memory of Arkady M. Galper and Nikolay P. Topchiev, who both recently passed away. They had been working in the field of experimental high-energy astrophysics and cosmic rays for nearly 70 and 50 years, respectively. They will always be remembered as enthusiastic scientists and great supervisors, colleagues, and friends.

## Funding

This work was supported by the Russian Science Foundation, project no. 19-72-10161, <https://rscf.ru/en/project/19-72-10161/>.

## References

- Adriani, O., Barbarino, G.C., Bazilevskaya, G.A., et al., *PAMELA measurements of cosmic-ray proton and helium spectra*, *Science*, 332, Issue 6025, 69-72, 2011, supporting materials.
- Adriani, O., Barbarino, G.C., Bazilevskaya, G.A., et al., *The PAMELA Mission Heralding a new era in precision cosmic ray physics*, *PR* 544, 4, 323–370, 2014.
- Adriani, O., Barbarino, G.C., Bazilevskaya, G.A., et al., *Trapped proton fluxes at low Earth orbits measured by the PAMELA experiment*, *APJ*, V. 799, Issue 1:L4, 7 pp., 2015.
- Bruno, A., Martucci, M., Cafagna, F.S., et al., *East–West proton flux anisotropy observed with the PAMELA mission*, *ApJ*, 919, No 2, 6 pp., 2021a.
- Bruno, A., Martucci, M., Cafagna, F.S., et al., *Solar-cycle variations of South Atlantic Anomaly proton intensities measured with the PAMELA mission*, *ApJL*, 917, No 2, 6 pp., 2021b.
- Cook, W. R., Cummings, A.C., Cummings, J.R., et al., *MAST: a mass spectrometer telescope for studies of the isotopic composition of solar, anomalous, and galactic cosmic ray nuclei*, *IEEE Transactions on Geoscience and Remote Sensing*, 31, no. 3, 557–564, 1993.
- Giovacchini, F., Oliva, A., Valencia-Otero, M., *Observation of  $Z>2$  trapped nuclei by AMS on ISS*, DOI: 10.22323/1.395.1288, *PoS ICRC2021* 1288, 2022.
- Hudson, M.K., Kress, B.T., Mazur, J.E., et al., *3D modelling of shock-induced trapping of solar energetic particles in the Earth’s magnetosphere*, *J. Atmos. Sol. Terr. Phys.*, 66, 1389-1397, 2004.
- Kuznetsov, N. V., and Nikolayeva, N. I., *Empirical model of pitch-angle distributions of trapped protons on the inner boundary of the Earth’s radiation belt*, *Cosmic Research*, 50, 1, 13–20, 2012.
- Fiandrini, E., Esposito, G., Bertucci, B., et al., *Protons with kinetic energy  $E > 70$  MeV trapped in the Earth’s radiation belts*, *J. Geophys. Res.*, 109, A10214, 2004.
- Leonov, A., Cyamukungu, M., Cabrera, J., et al., *Pitch angle distribution of trapped energetic protons and helium isotope nuclei measured along the Resurs-01 No. 4 LEO satellite*, *Annales Geophysicae*, 23, no. 9, 2983–2987, 2005.
- Leonov, A.A., Galper, A.M., Koldashov, S.V., et al., *Inner radiation belt source of helium and heavy hydrogen isotopes*, *Adv. Space Res.*, 41, issue 1, 86–91, 2008.
- Fisher, H.M., Auschrat V.M., and Wibberenz, G., *Angular distribution and energy spectra of protons of energy  $5 < E < 50$  MeV at the lower edge of the radiation belt in equatorial latitudes*, *JGR*, V. 82, No 4, 537-547, 1977.
- Malakhov, V.V., & Mayorov, A.G., *Calculating a directional flux in near-Earth space*, *Bull. Russ. Acad. Sci. Phys.*, 85, No 4, pp. 386–388, 2021.
- Malakhov, V.V., Leonov, A.A., Mayorov, A.G., and V.V. Mikhailov, V.V., *Measurements of the trapped proton and helium fluxes in the PAMELA experiment*, DOI: 10.22323/1.444.0117, *PoS ICRC2023* 117, 2023.
- Malakhov, V.V., Leonov, A.A., Mayorov, A.G., and V.V. Mikhailov, V.V., *Calculation of geomagnetically trapped proton flux from the PAMELA experimental data*, DOI: 10.1134/S1063778824010356, *Phys. Atom. Nucl.*, V. 87 No. 1, pp. 226-233, 2024 in print.
- Martucci, M., Bartocci, S., Battiston, R., et al., *New results on protons inside the South Atlantic Anomaly, at energies between 40 and 250 MeV in the period 2018–2020, from the CSES-01 satellite mission*, *Phys. Rev. D*, 105, issue 6, 062001, 2022.
- Mazur, J.E., Blake, J.B., Slocum, P.L., et al., *The creation of new ion radiation belts associated with solar energetic particle events and interplanetary shocks*, in *Solar Eruptions and Energetic Particles*, *Geophys. Monogr. Ser.*, vol. 165, pp. 345–352, AGU, Washington, D. C., 2006.
- McIlwain, C.E., *Magnetic coordinates*, *Space Science Reviews*, 5, 585, 1966.

Parker, E.N., *Newtonian development of the dynamical properties of ionized gases of low density*, *Phys. Rev.*, 107, 924, 1957.

Picozza, P., Galper, A.M., Castellini, G., et al., *PAMELA – A payload for antimatter matter exploration and light-nuclei astrophysics*, *Astroparticle Physics* 27, 296–315, 2007.

X. Rederer, *Dynamic of radiation trapped by geomagnetic field*, Moscow, MIR, 1971.

Selesnick, R.S., Cummings, A.C., Cummings, J.R., et al., *Geomagnetically trapped anomalous cosmic rays*, *JGR*, V.100, No A6, 9503–9518, 1995.

Selesnick, R.S., Looper M.D., and Mewaldt, R.A., *A theoretical model of the inner proton radiation belt*, *Space Weather*, V. 5, Issue 4, 2007.

Singer, S.F., “*Radiation belt*” and trapped cosmic-ray albedo, V. 1, No 5, pp. 171-173, 1958.

Sullivan, J.D., *Geometric factor and directional response of single and multi-element particle telescopes*, *Nucl. Instrum. Methods* 95, issue 1, 5–11, 1971.

Zhang, Y.-L., Wang, X.-L., & Xu, Z.-Z., *Evaluation of particle acceptance for space particle telescope*, *Chinese Phys.*, C 35, 774-777, 2011.

### **Declaration of interests**

☒ The authors declare that they have no known competing financial interests or personal relationships that could have appeared to influence the work reported in this paper.

☐ The authors declare the following financial interests/personal relationships which may be considered as potential competing interests: